

# A LOW-ENERGY RF DEFLECTOR FOR THE FERMI@ELETTRA PROJECT

P. Craievich\*, S. Biedron, D. La Civita, M. Ferianis (Elettra, Trieste, Italy)  
 M. Petronio, R. Vescovo (DEEI, Università degli Studi di Trieste, Trieste, Italy)  
 D. Alesini, L. Palumbo (Laboratori Nazionali di Frascati, INFN/LNF, Roma, Italy)  
 L. Ficcadenti (Università la Sapienza Roma, Roma, Italy)

## Abstract

A RF deflector is a useful tool to completely characterize the beam phase space by means of measurements of the bunch length and the transverse slice emittance. At FERMI@Elettra, a soft X-ray next-generation light source under development at the Sincrotrone Trieste laboratory in Trieste, Italy, we are installing low-energy and high-energy deflectors. In particular, two deflecting cavities will be positioned at two points in the linac. One will be placed at 1.2 GeV (high energy), just before the FEL process starts; the other at 250 MeV (low energy), after the first bunch compressor (BC1). This paper concerns only the low-energy deflector. The latter was built over the past year in collaboration with the SPARC project team at INFN-LNF-Frascati, Italy and the University of Rome. In this paper we will describe the RF measurements performed to characterize the standing wave cavity before the installation in the FERMI@Elettra linac, and we will compare them with the simulations done using the electromagnetic code HFSS.



Figure 1: The low energy deflector in the FERMI@Elettra Linac.

## INTRODUCTION

The RF deflector is a five cell standing wave structure, which has been installed in the FERMI@Elettra linac after the BC1 bunch compressor (Fig. 1). The cavity shares the same klystron (K1) of the electron gun, thus an attenuator and a phase shifter, placed in the deflector arm, are required to independently modulate the input power, as is shown in Fig. 2. The RF power travels from K1 to a sixty meters rectangular waveguide, which is connected to the cavity with a taper. Six vacuum pumps in the rectangular waveguide monitor the vacuum trends, while another vacuum pump ( $P_7$ ) has been placed near the cavity in the linear accelerator. The vacuum level reached the value  $5 \cdot 10^{-9}$  mbar two weeks after the cavity installation without input power. A RF setup which allows the estimation of the input power and of the behavior of the cavity using diodes and directional couplers has already been implemented.

In the FERMI@Elettra project the low energy deflector will be used at 250 MeV as a beam diagnostic tool. The bunch length measurements performed by the RF cavity will evaluate the efficiency of the BC1 compressor. Furthermore the slice emittance and the beam energy measure-

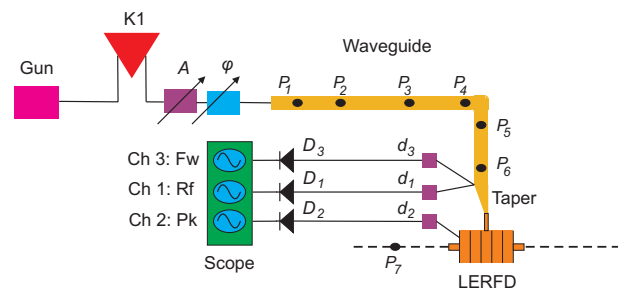


Figure 2: Schematic layout of the low energy deflector:  $A$  is the attenuator,  $\phi$  is the phase shifter,  $P_i$  is a vacuum pump ( $i = 1..7$ ),  $d_k$  and  $D_k$  are directional couplers and diodes, respectively ( $k=1..3$ ).

ments will be done by means of the layout shown in Fig. 3, which is composed by five quadrupoles, three OTR screens and the BC1 spectrometer.

The RF conditioning of the deflector has started during the last run of the FERMI@Elettra commissioning in June,

\* paolo.craievich@elettra.trieste.it

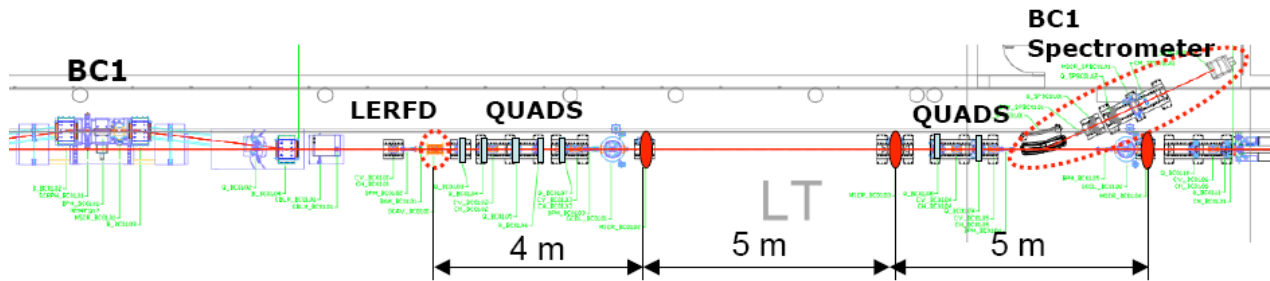


Figure 3: The low-energy RF deflector layout.

while the first beam measurements will take place within this year. In this first phase the vacuum level was approximately to  $2 \cdot 10^{-8}$  mbar with an input power of 1MW and a pulse length of  $0.6\mu s$ .

In this paper the RF design performed with HFSS [1] will be discussed, describing the procedure used to obtain field flatness and to properly excite the deflecting mode [2]. Then we will compare the RF parameters obtained with the code with the one calculated with the network analyzer using the bead-pull technique.

### RF DESIGN

The main constraints of the RF deflector have been the required integrated deflecting voltage  $V_t > 3$  MV, the working frequency  $f=2.99801$  GHz, the filling time  $t_F < 3\mu s$  and the input power available  $P_{in}=5$  MW [3]. The starting point of the RF design has been the basic cell, which is shown in Fig. 4. The main geometrical parameter are the the cell length  $L_{cell}$ , the iris radius  $a$ , the external radius  $R$  and the disk width  $t$ .

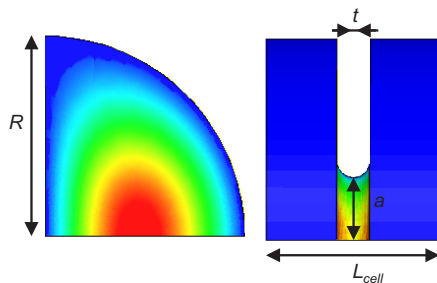


Figure 4: Electric field amplitude in the low energy deflector basic cell.

Using  $L_{cell}=50$  mm,  $a=18$  mm,  $t=9.5$  mm  $R=57.64$  mm the deflecting  $\pi$ -mode has been excited in the basic cell at the proper working frequency. The sensitivities of the geometrical parameters are reported in Table 1. As expected the external radius and the iris radius are the most important parameters for the mechanical tolerances.

The evaluation of the RF parameters in a five cell structure has been performed with the model shown in Fig. 5.

Setting all the external radius to  $R$ , a non-uniform magnetic field profile has been observed on axes, thus we var-

Table 1: Basic Cell Sensitivities.

$a$	-20.18 MHz/mm
$b$	-47.3 MHz/mm
$L$	2.1 MHz/mm
$t$	0.91 MHz/mm

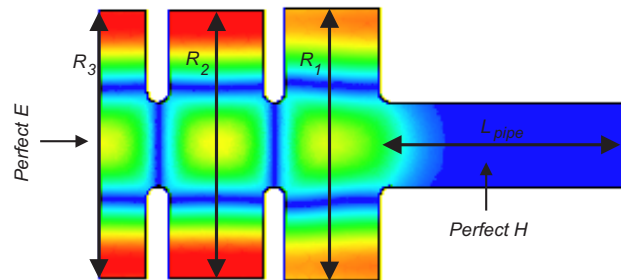


Figure 5: Magnetic field amplitude in the HFSS model used to evaluate the field flatness.

ied  $R_1$  to improve the field flatness. Moving the external radius from  $R_1 = 57.64$  to  $R_1 = 58.24$  we achieved for the normalized transversal magnetic field  $H_{t,n}$  the flatness  $F = 7\%$ , as is shown in Fig. 6.

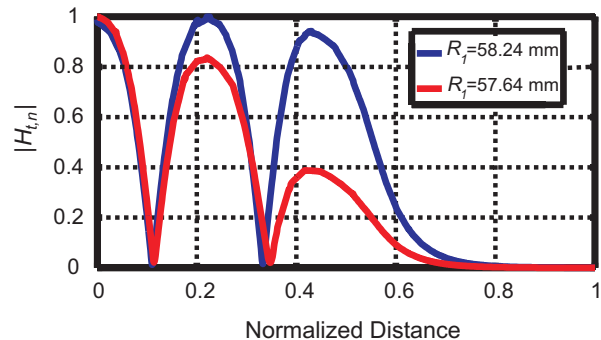


Figure 6: Normalized magnetic field amplitude on axis for different values of the external radius  $R_1$ .

The model in Fig. 5 have also been used to obtain the resonant frequencies of the five cell structure. If the bound-

ary condition in the half of middle cell is a perfect electric conductor, only the modes which are excitable by the coupler ( $\pi$ ,  $\frac{3}{5}\pi$  and  $\frac{2}{5}\pi$ ) can be found. The other resonant modes ( $\frac{4}{5}\pi$  and  $\frac{1}{5}\pi$ ) have been obtained using a perfect magnetic conductor as a boundary condition in the half of middle cell. The results are reported in Table 2.

Table 2: Resonant modes frequencies measured obtained with HFSS

$f_\pi$	2.9976 GHz
$f_{\frac{4}{5}\pi}$	3.0045 GHz
$f_{\frac{3}{5}\pi}$	3.0281 GHz
$f_{\frac{2}{5}\pi}$	3.0663 GHz
$f_{\frac{1}{5}\pi}$	3.1090 GHz

The frequency shifts of the nearest modes are  $\Delta f_1 = f_{\frac{4}{5}\pi} - f_\pi = 6.9$  MHz and  $\Delta f_2 = f_{\frac{3}{5}\pi} - f_\pi = 30.5$  MHz.

The excitation of the  $\pi$ -mode has been obtained varying simultaneously the middle radius  $R_1$  and  $x_w$  in the model in Fig. 7. Choosing  $R_3 = 57.45$  mm and  $x_w = 19.5$  mm, and slightly moving  $R_2$  to 57.6 mm and  $R_3$  to 58.25 mm to optimize the coupling, we found a coupling coefficient  $\beta = 1.08$  corresponding to a scattering parameter  $s_{11} = -27.8$  db. The final geometrical and RF parameters of the five cells structure have been reported in table 3, where  $R_t$  is the transverse shunt resistance and  $V_t = 4.9$  MV is the integrated deflecting voltage achievable with the maximum input power  $P_{in} = 5$  MW. The required deflecting voltage  $V_t = 3$  MV can be reached with an input power  $P_{in} = 1.9$  MW and a maximum electric peak of  $E_p = 48$  MV/m.

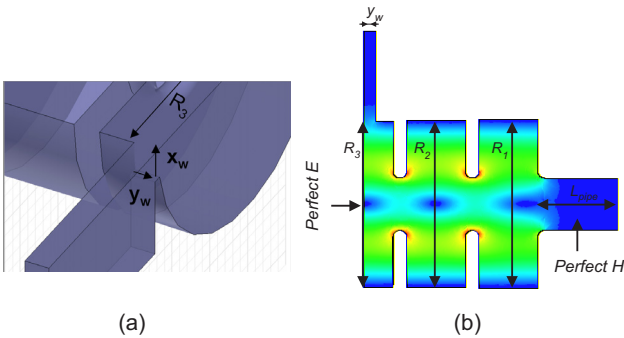


Figure 7: (a) Coupler detail (b) Electric field amplitude in the HFSS model used to evaluate the excitation of the deflecting mode.

## BEAD-PULL MEASUREMENTS

The low energy deflector has been realized and brazed at INFN/LNF workshops, where the first RF measurements with the network analyzer have been done. Then the cavity has been installed in FERMI@Elettra project in December 2009, where further tests and the final tuning have taken

Table 3: Main RF and geometrical parameters of the low energy deflector.

$L_{cell}$	50.00 mm	$f$	2.998 GHz
$R_1$	58.25 mm	$Q_0$	15600
$R_2$	57.60 mm	$R_t$	2.4 M $\Omega$
$R_3$	57.45 mm	$R_t/Q_0$	156 $\Omega$
$a$	18 mm	$t_F$	2.4 $\mu$ s
$y_w$	8 mm	$V_t @ 5$ MW	4.9 MV
$x_w$	19.5 mm	$s_{11}$	-27.8 dB
$t$	9.5 mm	$\beta$	1.08

place; the room temperature was 20.7°C. Fig. 8 shows the transmission coefficient between two pick-ups placed in the two external cells. The five resonances observed are reported in Table 4.

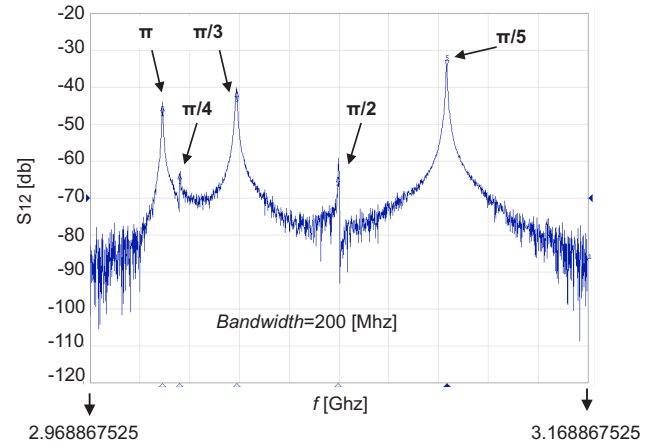


Figure 8: Resonant modes in the low energy deflector.

Table 4: Resonant modes frequencies measured with the network analyzer.

$f_{r,\pi}$	2.99802 GHz
$f_{r,\frac{4}{5}\pi}$	3.00492 GHz
$f_{r,\frac{3}{5}\pi}$	3.02773 GHz
$f_{r,\frac{2}{5}\pi}$	3.06856 GHz
$f_{r,\frac{1}{5}\pi}$	3.11219 GHz

We can see that the frequency shifts  $\Delta f_{r,1} = f_{r,\frac{4}{5}\pi} - f_{r,\pi} = 6.9$  MHz and  $\Delta f_{r,2} = f_{r,\frac{3}{5}\pi} - f_{r,\pi} = 29.7$  MHz have approximately the same values of  $\Delta f_1$  and  $\Delta f_2$ , which have been predicted by HFSS. We measured the load quality factor  $Q_l$  of the deflecting mode evaluating the  $s_{12}$  transmission coefficient between the input coupler and one pick-up. Then we obtain the coupling coefficient  $\beta$  measuring the  $s_{11}$  coefficient from the input coupler. Thus we was able to calculate the unloaded quality factor as  $Q_0 =$

$Q_l(1 + \beta)$  and the external quality factor as  $Q_{ext} = Q_0/\beta$ . The filling time has been calculated as  $t_F = 3\tau$ , where  $\tau = \frac{2Q_l}{2\pi f}$ . The experimental results and the predicted value are reported in in Table 5.

Table 5: Comparison between the RF parameters simulated and measured.

	HFSS	Measured
$\beta$	1.08	1.1
$Q_0$	15600	14600
$Q_l$	7090	6900
$Q_{ext}$	14300	13200
$\tau[\mu s]$	0.8	0.74
$s_{11}$	-27.8	-26.3

We can observe that a good agreement has been found between the RF parameters obtained with HFSS and the experimental parameters, which are very close to the predicted values.

In order to evaluate the field flatness, we used the bead pull technique [4]. Thus we moved a small bead attached to a thin nylon line through the cavity, evaluating the frequency shift of the deflecting mode, which is proportional to the square of the local field. In particular we evaluate the phase  $\Delta\phi$  of the coefficient  $s_{12}$ , which is proportional to frequency shift due to the perturbation. The measurement was first performed with a metallic sphere, which perturb both the electric and the magnetic field. Then we used a dielectric cylinder, which affects only the electric field. Since in the middle of the iris the magnetic field is zero, the perturbation introduced by the metallic sphere is completely given by the electric field. For that reason the two traces can be normalized using the maximum value of  $\Delta\phi$  in the middle of the iris. Subtracting the squares of the normalized traces we obtained the results shown in Fig. 9; the field flatness achieved is  $F = 6\%$ .

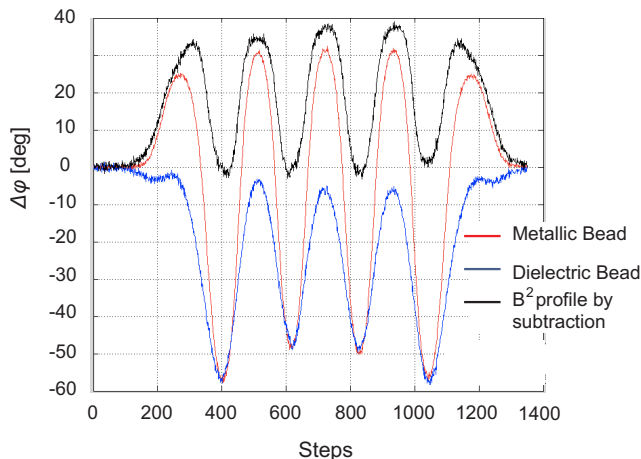


Figure 9: Flatness field obtained with bead pull measurements.

After having tested field flatness, the cavity has finally been tuned to the working frequency  $f=2.998.01$  GHz in vacuum using the cooling system and the tuners.

## CONCLUSION

In this paper the complete RF design of the low energy deflector has been reported. The RF measurements performed at the FERMI@Elettra laboratory confirm the values predicted by the electromagnetic code HFSS. In the next months, we will continue the RF conditioning of the cavity and the first bunch measurements will take place.

## ACKNOWLEDGMENTS

The PhD of M. Petronio in the "Dipartimento di Elettrotecnica, Elettronica e Informatica" (DEEI) of the University of Trieste, Italy, is supported by Sincrotrone Trieste S.C.p.A., Italy.

## REFERENCES

- [1] [www.ansoft.com](http://www.ansoft.com)
- [2] Ficcadenti et al. "Electromagnetic design of the low energy RF Deflector for the FERMI@ELETTRA Project", talk held at Frascati, October 2007.
- [3] P. Craievich et al. *Fermi Low-Energy Transverse RF Deflector*, Proc. of Epac 2008, Genoa, Italy, June 23-27 2008, pp. 1239-1241.
- [4] L.C. Maier Jr. and J.C. Slater, *Field strength measurement in resonant cavities*, Journal of Applied Physics, 23, 1 (1951).